

Measurement of W- and Z-boson production in p-Pb collisions at $\sqrt{s_{\text{NN}}} = 5.02$ TeV with ALICE at the LHC

Jianhui Zhu^{1,2}, on behalf of the ALICE collaboration

¹Key Laboratory of Quark and Lepton Physics (MOE) and Institute of Particle Physics, Central China Normal University, Wuhan, China

²SUBATECH, Ecole des Mines de Nantes, Université de Nantes, CNRS-IN2P3, Nantes, France

E-mail: Jianhui.Zhu@cern.ch

Abstract. In hadronic collisions, electroweak bosons (W and Z) are produced in initial hard scattering processes and they are not affected by the strong interaction. In proton-proton collisions, they have been suggested as standard candles for luminosity monitoring and their measurement can improve the evaluation of detector performances. In nucleus-nucleus and proton-nucleus collisions, electroweak bosons provide a check at first order the validity of binary collision scaling, while small deviations allow studying the nuclear modifications of parton distribution functions. In ALICE, the production of W and Z bosons is measured via the contribution of W-boson decays to the inclusive p_{T} -differential muon yield and the invariant mass of unlike-sign muon pairs from Z-boson decays, respectively, at large rapidities. This paper reports on the production cross sections of muons from W muonic decay and of Z boson in p-Pb collisions at $\sqrt{s_{\text{NN}}} = 5.02$ TeV, which are compared to the theoretical calculations, and on the W-boson yields normalized to the average number of binary nucleon-nucleon collisions as a function of the event activity.

1. Introduction

The high collision energies available at the Large Hadron Collider (LHC) at CERN allow for an abundant production of hard probes, such as heavy quarks, quarkonia, high p_{T} jets and electroweak bosons (W^{\pm} , Z^0). Due to large masses of electroweak bosons, they are produced in initial hard parton scattering processes, with a formation time of the order of $1/M \sim 0.002 - 0.003$ fm/c and, having a lifetime of 0.08-0.10 fm/c, thus decay before the formation of the quark-gluon plasma (QGP), which is a deconfined phase of QCD matter that is formed in high-energy heavy-ion collisions. Furthermore, their leptonic decay products do not interact strongly with the hot and dense QCD medium. In proton-proton collisions, precise theoretical predictions of the W- and Z-boson production make them good standard candles for the luminosity measurement. Moreover, they can be used to constrain the parton distribution functions (PDFs) at high momentum transfer (Q^2). In proton-nucleus and nucleus-nucleus collisions, precise measurements of W- and Z-boson production can constrain the modification of the parton distribution functions in the nucleus (nPDFs) [1] and at first order they can be used to test the scaling of hard particle production with the number of binary nucleon-nucleon collisions [2].

2. Experimental apparatus and data sample

The ALICE experiment is equipped with two magnets and various detectors for triggering, tracking and particle identification [3, 4]. Muons are reconstructed in the muon spectrometer, which covers the pseudo-rapidity range $-4 < \eta_{\text{lab}} < -2.5$, consists of a thick front absorber, a dipole magnet, five tracking stations, a muon filter and two trigger stations. The inner tracking system consists of six layers of silicon detectors covering the range $|\eta_{\text{lab}}| < 0.9$. In this analysis, the interaction vertex is measured with the two innermost layers, which are equipped with Silicon Pixel Detectors (SPD). The number of clusters in the outer layer of the SPD (CL1) can be used to characterize the event activity. Two arrays of scintillators placed at both sides of the interaction point, the VZERO detector (V0A ($2.8 < \eta_{\text{lab}} < 5.1$) and V0C ($-3.7 < \eta_{\text{lab}} < -1.7$)), provide the trigger and an additional event activity estimation. A third estimation of the event activity is obtained with the Zero Degree Calorimeters (ZNA and ZNC) located at both sides of the detector at 112.5 m from the main interaction point along the beam line. Due to the energy asymmetry of the proton and lead colliding beams at the LHC, the centre-of-mass system of nucleon-nucleon collisions is shifted by $\Delta y = 0.465$ in the direction of the proton beam, with respect to the laboratory frame. Experimental data have been collected with two beam configurations (p-Pb and Pb-p) by inverting the orbits of the two particle species. The rapidity regions covered by the muon spectrometer in the two cases are $2.03 < y_{\text{cms}}^{\mu} < 3.53$ (forward, p-going direction) and $-4.46 < y_{\text{cms}}^{\mu} < -2.96$ (backward, Pb-going direction).

The data have been collected at $\sqrt{s_{\text{NN}}} = 5.02$ TeV with minimum bias (MB), high- p_{T} single-muon (MSH) and low- p_{T} di-muon (MUL) triggers. The MB trigger is defined requiring hits in both sides of the VZERO detector in coincidence with the beam counters. The MSH trigger is defined by asking, in addition to the MB condition, for a high transverse momentum muon with $p_{\text{T}} \gtrsim 4.2$ GeV/c in the trigger system of the spectrometer. The MUL is a coincidence of MB trigger and an unlike-sign muon pair selected with $p_{\text{T}} \gtrsim 0.5$ GeV/c for each of them. The MSH and MUL data samples are used for W- and Z-boson analysis, respectively. The integrated luminosity for the forward and backward rapidity measurements are 5.03 ± 0.18 nb $^{-1}$ and 5.81 ± 0.20 nb $^{-1}$ [5], respectively. The track in the muon tracking system is required to be in the geometrical acceptance ($-4 < \eta_{\text{lab}} < -2.5$), to have a polar angle measured at the end of the front absorber of $170^{\circ} < \theta_{\text{abs}} < 178^{\circ}$ and match a tracklet in the trigger stations in order to reject the remaining contamination from hadrons. Furthermore, the correlation between momentum and distance of closest approach (DCA) to the interaction vertex was used to remove beam-gas collisions and secondary particles produced in the absorber.

3. W-boson measurement

The present analysis is based on the extraction of the W-boson contribution from the transverse momentum distribution of inclusive muons. At high p_{T} , the main contributions to the yield of inclusive muons come from the muonic decays of W bosons, the di-muon decays of Z^0/γ^* bosons and the semi-muonic decays of beauty hadrons. The yield of muons from W-boson decays can be obtained through a fit based on suitable parameterizations of the different components. The distribution of muons from intermediate vector boson decays is described by Monte Carlo (MC) templates obtained from POWHEG simulations [6]. The isospin dependence of the W-boson differential cross-section [7] is accounted for by simulating separately p-p and p-n collisions and then summing the results together according to:

$$\frac{1}{N_{\text{p-Pb}}} \cdot \frac{dN_{\text{p-Pb}}}{dp_{\text{T}}} = \frac{Z_{\text{Pb}}}{A_{\text{Pb}}} \cdot \frac{1}{N_{\text{p-p}}} \cdot \frac{dN_{\text{p-p}}}{dp_{\text{T}}} + \frac{A_{\text{Pb}} - Z_{\text{Pb}}}{A_{\text{Pb}}} \cdot \frac{1}{N_{\text{p-n}}} \cdot \frac{dN_{\text{p-n}}}{dp_{\text{T}}} \quad (1)$$

where $A_{\text{Pb}} = 208$ and $Z_{\text{Pb}} = 82$. The generation of muons from Z^0/γ^* decays is performed in an equivalent way. For the description of the background at low p_{T} ($10 < p_{\text{T}} < 40$ GeV/c), which originates from the decays of beauty hadrons, three approaches are adopted: MC templates

83 based on pQCD calculations with FONLL [8], functional form, which was already successfully
 84 adopted for analogous measurements by the ATLAS experiment at the LHC [9] and another
 85 function derived from the second term of the parameterization used by ATLAS, which can be
 86 written as $f(p_T) = a \cdot \frac{e^{b \cdot \sqrt{p_T}}}{p_T^c}$. The different contributions are summed together in the fit function:

$$f(p_T) = N_{\mu \leftarrow \text{HF}} \cdot f_{\mu \leftarrow \text{HF}}(p_T) + N_{\mu \leftarrow W} \cdot f_{\mu \leftarrow W}(p_T) + N_{\mu \leftarrow Z^0/\gamma^*} \cdot f_{\mu \leftarrow Z^0/\gamma^*}(p_T) \quad (2)$$

87 where $f_{\mu \leftarrow \text{HF}}$ can be either a functional form or the MC template for muons from heavy-flavour
 88 decays, and $f_{\mu \leftarrow W}$ and $f_{\mu \leftarrow Z^0/\gamma^*}$ are the MC templates for muons from W and Z^0/γ^* boson
 89 decays, respectively. The number of muons from W decays ($N_{\mu \leftarrow W}$) is a free parameter, while
 90 the ratio $N_{\mu \leftarrow Z^0/\gamma^*}/N_{\mu \leftarrow W}$ is fixed to the value obtained with POWHEG. Figure 1 presents
 91 three examples of the combined fit for μ^+ by varying heavy-flavour background description.

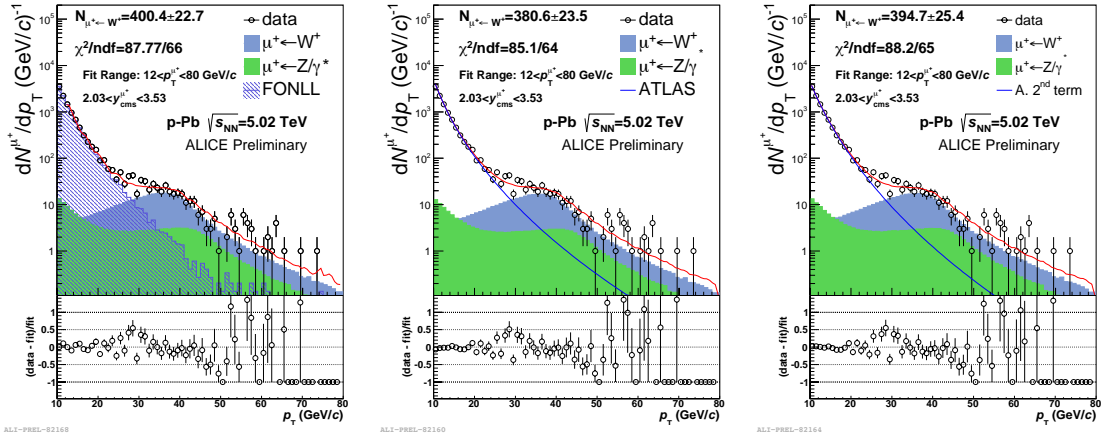


Figure 1. Examples of the combined fit to the inclusive p_T -spectrum of μ^+ at forward rapidity. Heavy-flavour templates based on FONLL [8] (left), the ATLAS function [9] (middle) and the 2nd term (second addend) of the ATLAS function (right). The errors on the yields represent the statistical uncertainties.

92 The uncertainty on the background description is determined by using either FONLL-based
 93 MC templates or functional forms and by varying the p_T range in the fit. The relative
 94 contribution of Z^0/γ^* is varied based on POWHEG and PYTHIA [10] predictions. The effect of
 95 the detector alignment is taken into account by producing the templates using different residual
 96 alignment assumptions. The signal was extracted several times by varying the above conditions
 97 and the final result is chosen as the weighted average of all of the trials. The systematic
 98 uncertainties are given by the RMS of the trials. It is worth noting that POWHEG does not
 99 account for the nuclear modification of the PDFs. Hence, the signal extraction using PYTHIA
 100 with EPS09 parameterization of the nuclear PDFs [11] was included in the calculation of the
 101 systematic uncertainties.

102 After signal extraction, the yields of muons from W-boson decays are corrected for acceptance
 103 times efficiency (88% for forward, 76% for backward). The measured production cross-sections
 104 of muons from W-boson decays at forward and backward rapidity in p-Pb collisions are shown
 105 in Figure 2 and compared with theoretical predictions based on NLO pQCD calculations with
 106 CT10 PDFs [12] and modified CT10 PDFs with the EPS09 parametrization of nuclear effects.
 107 Both of the theoretical predictions with and without EPS09 agree with the measurement within
 108 uncertainties.

109 The yield of muons from W-boson decays can also be extracted per event activity interval.
 110 It is corrected for acceptance times efficiency and normalized to the number of equivalent MB

111 event. Thus, the normalized yield can be divided by the average number of binary nucleon-
 112 nucleon collisions $\langle N_{\text{coll}} \rangle$ in each event activity interval, in order to obtain the yield per binary
 113 collision. The average number of binary collisions $\langle N_{\text{coll}} \rangle$ is determined from a Glauber-model
 114 based analysis in the case of V0A, V0C and CL1 estimators, while for the ZN estimator it
 115 is computed with a hybrid approach, assuming that the particle density at mid-rapidity is
 116 proportional to the number of nucleons participating in the collision, N_{part} [2]. The measured
 117 yields of muons from W-boson decays over $\langle N_{\text{coll}} \rangle$ in p-Pb collisions at forward and backward
 118 rapidities are shown in Figure 3 as a function of event activity. The results present a flat trend
 119 as function of event activity, and are similar for the three estimators within uncertainties.

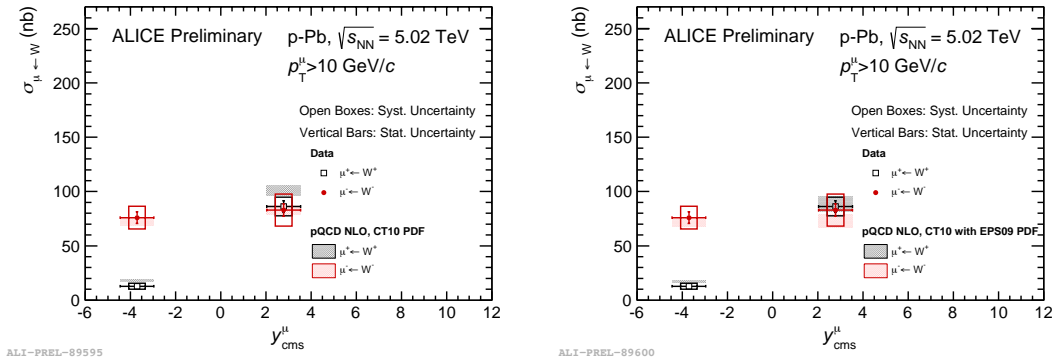


Figure 2. The cross section of muons from W-boson decays compared with pQCD [1] calculations with CT10 PDFs [12] (left) and CT10 PDFs including nuclear effects EPS09 [11] (right) at forward and backward rapidity. The cut of $p_T > 10$ GeV/c is added.

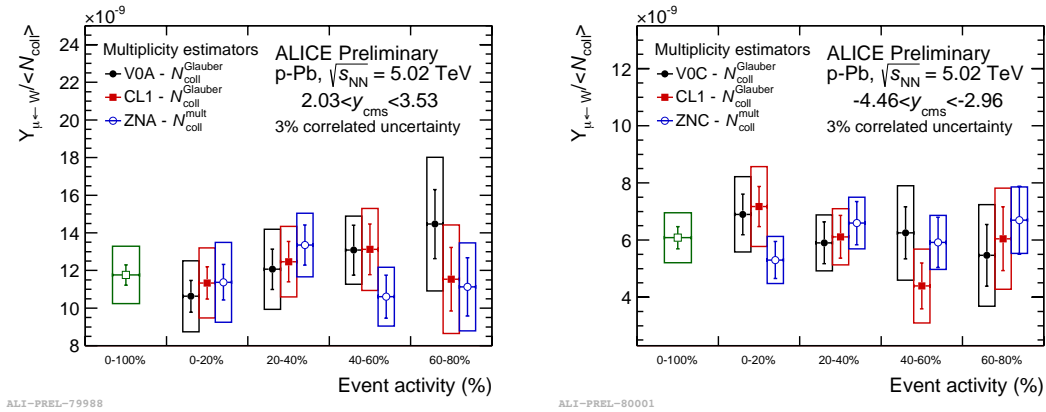


Figure 3. Muon yields from W-boson decays normalized to the average number of binary collisions as a function of event activity at forward (left) and backward (right) rapidity. The green points represent the values in minimum-bias collisions.

120 4. Z-boson measurement

121 The signal of Z boson is seen as a peak around 90 GeV/c² in the invariant-mass distribution
 122 of unlike-sign muon pairs, selected according to the criterion described in section 2 and with

123 $p_T > 20$ GeV/c in order to reduce background from lower mass resonances decay and of the
 124 semi-leptonic decay of charm and beauty hadrons. It was verified that loosening the requirement
 125 on the minimum p_T of the muons to 10 GeV/c does not introduce any additional unlike-sign
 126 muon pair with $m_{\mu\mu} > 40$ GeV/c². The invariant mass distribution is shown in Figure 4. 22
 127 (2) candidates with $m_{\mu\mu} > 60$ GeV/c² were reconstructed at forward (backward) rapidity in
 128 p-Pb collisions. At forward rapidity, the distribution is compared with expectations from the
 129 POWHEG simulations with CT10 PDFs and EPS09 nPDFs. The parameters were extracted
 130 from a fit using the Crystal-Ball function [13], which consists of a Gaussian core with power-
 131 law tails on both sides. A good agreement within the experimental uncertainties between
 132 data and POWHEG is obtained. The contribution to the invariant-mass distribution from
 133 the combinatorial background can be estimated using the like-sign dimuon distribution: no
 134 candidates were found in the region $60 < m_{\mu\mu} < 120$ GeV/c². A 0.1% upper limit for this
 135 contribution is obtained by extrapolating the like-sign dimuon distribution at low mass to the
 136 region of interest. Contributions from other physics processes, like the semi-leptonic decay of $c\bar{c}$,
 137 $b\bar{b}$ and $t\bar{t}$ pairs and the muonic decay of τ pairs in the process ($Z \rightarrow \tau\tau \rightarrow \mu\mu$), is estimated using
 138 MC simulations to be less than 0.7% (0.4%) at forward and backward rapidity, respectively.

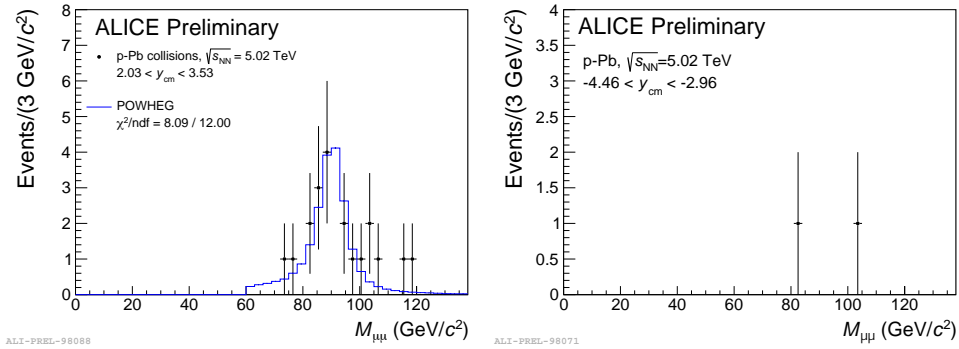


Figure 4. Invariant-mass distribution of unlike-sign muon pairs with $p_T > 20$ GeV/c in the p-going (left panel) and Pb-going (right panel) direction. The blue line represents the distribution obtained using POWHEG simulation with CT10 PDFs and EPS09 nPDFs and normalized to the number of Z candidates in the data.

139 The measured number of candidates is corrected by the acceptance times efficiency (78%
 140 for forward, 61% for backward) with a relative systematic uncertainty (1% for forward, 2% for
 141 backward). The measured production cross section of muons from Z-boson decays at forward
 142 and backward rapidity in p-Pb collisions is shown in Figure 5 (left) and compared with next-to-
 143 next-to leading order (NNLO) Fully Exclusive W and Z (FEWZ) [14] predictions with CT10nlo
 144 [15], CTEQ6m [16], JR09NNLO [17] and MSTW2008NNLO [18] with and without nPDFs. Since
 145 there are few candidates at backward rapidity, limiting the measurement statistical precision,
 146 an upper limit of the cross section is also evaluated. The ratio of the measured cross sections
 147 (obtained by ALICE and LHCb [19]) to FEWZ are shown in Figure 5 (right). The measurements
 148 of ALICE are in agreement with theoretical calculations at both rapidity regions.

149 5. Conclusion

150 The production cross section of muons from W- and Z-boson decays at forward and backward
 151 rapidity has been measured in p-Pb collisions at $\sqrt{s_{NN}} = 5.02$ TeV with the ALICE muon
 152 spectrometer. Theoretical predictions based on NLO pQCD and FEWZ calculations with CT10
 153 PDFs agree with the measurement within uncertainties for W and Z boson, respectively. Taking
 154 into account the EPS09 parametrization of nuclear effects on the PDFs further improves the

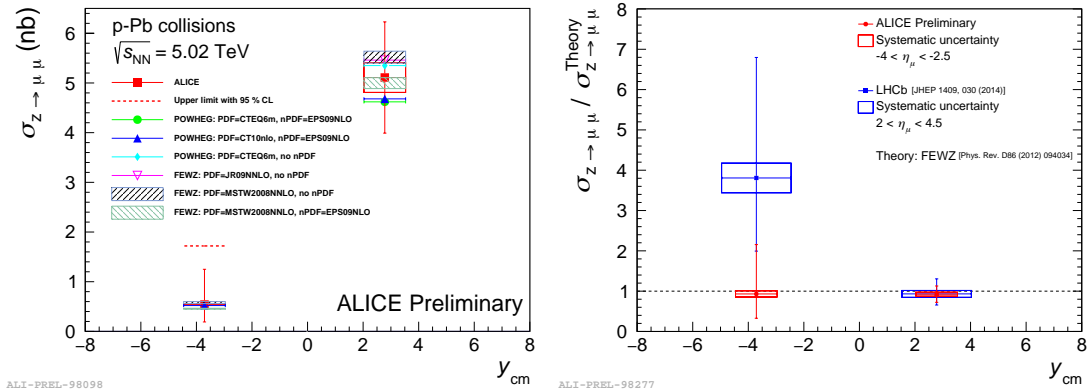


Figure 5. (Left) The cross section of muons from Z-boson decays compared to FEWZ [14] calculations with different PDFs with and without nuclear effects EPS09 [11]. (Right) The ratio of cross section to FEWZ calculation measured by the ALICE collaboration is compared with those obtained by the LHCb collaboration [19].

155 agreement between theoretical predictions and the measurements at forward rapidity where
 156 shadowing is expected to be important. The ALICE measurement on Z-boson agrees with the
 157 results from LHCb [19] at forward and backward rapidities, whereas CMS [20, 21] and ATLAS
 158 [22] results indicate that electroweak bosons favour the modification of the PDFs at mid-rapidity.
 159 The yield of muons from W-boson decays in different event activity scales with $\langle N_{coll} \rangle$ within
 160 the experimental uncertainties.

161 Acknowledgments

162 This work is supported partly by the Chinese Ministry of Science and Technology 973
 163 grant 2013CB837803, NSFC Grant 11375071, 11475068, IRG 11521064 and CSC grant No.
 164 201306770033.

165 References

- 166 [1] Paukkunen H and Salgado C A 2011 *JHEP* **03** 071
 167 [2] Adam J *et al.* (ALICE Collaboration) 2015 *Phys. Rev. C* **91** 064905
 168 [3] Aamodt K *et al.* (ALICE Collaboration) 2008 *JINST* **3** S08002
 169 [4] Abelev B *et al.* (ALICE Collaboration) 2014 *Int. J. Mod. Phys. A* **29** 1430044
 170 [5] Adam J *et al.* (ALICE Collaboration) 2015 *JHEP* **11** 127
 171 [6] Alioli S, Nason P, Oleari C and Re E 2008 *JHEP* **07** 060
 172 [7] Conesa del Valle Z, CERN-THESIS-2007-102
 173 [8] Cacciari M, Greco M and Nason P 1998 *JHEP* **05** 007
 174 [9] Aad G *et al.* (ATLAS Collaboration) 2011 ATLAS-CONF-2011-078
 175 [10] Sjostrand T, Mrenna S and Skands P 2006 *JHEP* **05** 026
 176 [11] Eskola K J, Paukkunen H and Salgado C A 2009 *JHEP* **04** 065
 177 [12] Lai H L *et al.* 2010 *Phys. Rev. D* **82** 074024
 178 [13] Gaiser J 1982 PhD thesis (<http://www.slac.stanford.edu/cgi-wrap/getdoc/slac-r-255.pdf>)
 179 [14] Gavin R, Li Y, Petriello F and Quackenbush S 2011 *Comput. Phys. Commun.* **182** 2388-2403
 180 [15] Lai H L, Guzzi M, Huston J, Li Z, Nadolsky P M, Pumplin J and Yuan C P 2010 *Phys. Rev. D* **82** 074024
 181 [16] Nadolsky P M *et al.* 2008 *Phys. Rev. D* **78**(1) 013004
 182 [17] Jimenez-Delgado P and Reya E 2009 *Phys. Rev. D* **79** 074023
 183 [18] Martin A D, Stirling W J, Thorne R S and Watt G 2009 *Eur. Phys. J. C* **63** 189-285
 184 [19] Aaij R *et al.* (LHCb Collaboration) 2014 *JHEP* **09** 030
 185 [20] Khachatryan V *et al.* (CMS Collaboration) 2015 *Phys. Lett. B* **750** 565-586
 186 [21] Khachatryan V *et al.* (CMS Collaboration) 2016 *Phys. Lett. B* **759** 36-57
 187 [22] Aad G *et al.* (ATLAS Collaboration) 2015 *Phys. Rev. C* **92** 044915